Multifunctional Hybrid Nanogel for Integration of Optical Glucose Sensing and Self-Regulated Insulin Release at Physiological pH

Weitai Wu,[†] Nivedita Mitra,[‡] Elsa C. Y. Yan,[‡] and Shuiqin Zhou[†,*]

[†]Department of Chemistry, College of Staten Island of The City University of New York, 2800 Victory Boulevard, Staten Island, New York 10314 and [‡]Department of Chemistry, Yale University, 225 Prospect Street, New Haven, Connecticut 06520

ABSTRACT Optical detection of glucose, high drug loading capacity, and self-regulated drug delivery are simultaneously possible using a multifunctional hybrid nanogel particle under a rational design in a colloid chemistry method. Such hybrid nanogels are made of Ag nanoparticle (NP) cores covered by a copolymer gel shell of poly(4-vinylphenylboronic acid-*co*-2-(dimethylamino)ethyl acrylate) [p(VPBA—DMAEA)]. The introduction of the glucose sensitive p(VPBA—DMAEA) gel shell onto Ag NPs makes the polymer-bound Ag NPs responsive to glucose. While the small sized Ag cores (10 ± 3 nm) provide fluorescence as an optical code, the responsive polymer gel shell can adapt to a surrounding medium of different glucose concentrations over a clinically relevant range (0—30 mM), convert the disruptions in homeostasis of glucose level into optical signals, and regulate release of preloaded insulin. This shows a new proof-of-concept for diabetes treatment that exploits the properties from each building block of a multifunctional nano-object. The highly versatile multifunctional hybrid nanogels could potentially be used for simultaneous optical diagnosis, self-regulated therapy, and monitoring of the response to treatment.

KEYWORDS: silver nanoparticles · glucose-sensitive nanogels · nanobiosensor · insulin delivery · multifunctional

Significant advances have been achieved in the synthesis and modification of the inorganic nanoparticles (NPs) for biomedical applications. These nanosized materials offer a robust framework in which two or more functional building blocks can be incorporated to give multiple functionalities. For example, molecularly mediated assembly of noble metals such as Ag and Au NPs has been used for designing sensors, bioprobes, imaging diagnosis, and photothermal cancer therapy.[1−5] To sustain life and maintain biological function, nature requires systems that can offer multiple specific abilities in response to their surrounding environments. While noble metal NPs exhibit size-, shape-, and interdistance-dependent optical, electronic, and photothermal conversion properties,[1−7] they generally lack sensitivity to local environment change. Smart polymers that can undergo conformational and chemical changes in response to external stimuli, such as temperature, pH, or glucose level,[8−11] are often prepared for a broad range of application. Noble metal NPs coated with smart polymers can adapt to surrounding environments, convert chemical and biochemical signals (*e.g.*, disruptions in temperature and/or pH homeostasis that are associated with pathological zone)[12,13] into optical signals,[14−16] capture the analyte close to noble metal NPs for surface-enhanced Raman scattering analysis,[17] and regulate the release of preloaded drug.[18] The capability of simultaneous optical diagnosis and therapy with NPs may prove to be advantageous over conventional medicine.

In this text, we describe the construction of multifunctional hybrid nanogels that are designed for a combination of optical detection of glucose at physiological pH and temperature with self-regulated insulin release (Figure 1). There is an urgent need to develop a nanobiosensor for continuous glucose monitoring at physiological conditions in subjects with diabetes mellitus,[19] which represents one of the largest health concerns of the 21st century with worldwide prevalence. The most investigated methods for glucose measurement utilize the enzyme glucose oxidase. Although significant benefits have already been achieved, enzyme-based systems suffer from instabilities due to denaturation, difficulties associated with sterilization, and cost when used in a format suitable for continuous sensing.[19] This has led to considerable research interest in developing synthetic boronic acid ligands for binding and

*Address correspondence to shuiqin.zhou@csi.cuny.edu.

Received for review April 20, 2010 and accepted July 02, 2010.

Published online July 12, 2010.
10.1021/nn1008319

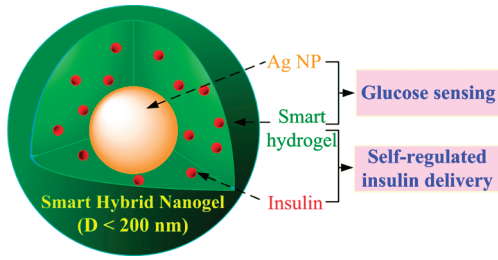

Figure 1. Schematic illustration of smart hybrid nanogels that can integrate optical glucose detection and self-regulated insulin delivery at physiological pH and temperature into a single nano-object.

detecting glucose.[20] These boronic acid-based ligands have been coupled with polymer for continuous glucose sensing,[9−11,21−26] including the holographic sensors based on the phenylboronic acid (PBA) copolymer film[21,25] and the photonic crystal glucose sensors based on the PBA-modified hydrogels.[22] While these glucose sensors exploited a change in diffraction or reflection, fluorescence-based systems are receiving increasing attention, encouraged by their special advantages for biological analysis with little or no damage to the host system. Different fluorescent organic moieties[19,27,28] and semiconductor quantum dots (QDs)[29−32] have been coupled with the boronic acid-based ligands. Techniques include measuring the changes in fluorescence resonance energy transfer (FRET) between a fluorescent donor and an acceptor because of competitive displacement,[29−31] and glucose-induced changes in intrinsic fluorescence of enzymes or extrinsic optical labels.[32] The advantages for QDs over organic fluorophores, including multicolor imaging, photostability, and high quantum yield, are significant, but the potential hazards caused by the release of cadmium are of serious concern.[33] An alternative to fluorophores or QDs for the labeling of glucose responsive polymers is the use of biocompatible noble metal NPs, because small sized noble metal NPs can offer strong and nonbleaching fluorescence.[34,35] Geddes's group reported a glucose sensor based on the Ag NPs capped with small molecules of thiolated boronic acid.[34] The interaction of glucose and dextran with thiolated boronic acid-capped silver nanoparticles in solution resulted in enhanced fluorescence intensity. On the other hand, the hydrogel beads, micro/nanogels, or mesoporous silica, offering the unique advantage of interior network structure for the incorporation of therapeutics, are being actively explored as carriers for insulin delivery.[10,36−40] To adjust treatment to maintain near-normoglycaemia, in some cases glucose-sensitive polymers are employed, and the release of insulin can be regulated by glucose-responsive swelling/shrinking of the polymer networks.[10,39] While a variety of monofunctional materials for either glucose detection or insulin delivery have been developed, unfortunately, to the best of our knowledge, no report of the multifunctional nanocarrier systems combining both optical glucose detection and insulin delivery has appeared in the literature. The combination of optical glucose with self-regulated insulin delivery into a single nano-object can potentially provide simultaneous diagnosis, therapy, and monitoring of the response to treatment.

Herein, we design a novel class of core−shell colloidal nanobiomaterials comprising small Ag NPs (10 ± 3 nm) coated with new boronate derivative, poly(4-vinylphenylboronic acid-*co*-2-(dimethylamino)ethyl acrylate) [p(VPBA−DMAEA)] nanogel network chains, as glucose recognition element. The p(VPBA−DMAEA) gel shell can undergo a volume phase transition in response to the change in glucose concentration with high sensitivity and selectivity over a clinically relevant range (0−30 mM) at the physiological pH and temperature upon a rational design of the polymer chains. While the small-sized Ag NP core can provide these hybrid nanogels with strong fluorescence, the glucose-induced swelling/shrinking of the p(VPBA−DMAEA) gel shell is expected to modify the physicochemical environment of the Ag NP core for manipulation of the fluorescence intensity, converting the variation in glucose level to optical signals. In addition to the signaling ability for glucose level change, we also demonstrated that these hybrid nanogel systems can modulate the delivery of preloaded insulin as a function of glucose level. The ability to track drug-loaded NPs in biological systems, optically detect glucose level, and intelligently dose the insulin of the multifunctional hybrid nanogels may hasten the development of more efficacious systems toward a good diabetic control.

RESULTS AND DISCUSSION

Following the main objective to probe glucose level and deliver insulin under physiological pH and temperature conditions, our strategy to prepare these novel multifunctional hybrid nanogels is based on a combination of several methods previously developed in both inorganic NP and polymer synthesis. First, the synthesis of noble metal NPs with controlled size, shape, and thus unique optical properties has been well established by several groups.[6,7] Second, while various boronic acid-based glucose recognition elements have been intensively developed,[19−22] our group and other groups have previously employed poly(*N*-isopropylacrylamide-*co*-phenylboronic acid), poly(*N*-isopropylacrylamide-*co*-acrylamide-*co*-phenylboronic acid) and other poly(*N*-isopropylacrylamide) based polymers to fabricate polymeric micro/nanogel with glucose-induced volume phase transition profiles.[9−11] Third, we have recently reported the buildup of temperature and pH sensitive poly(*N*-isopropylacrylamide-*co*-acrylic acid) shell on CTAB-capped Ag NPs (36 ± 3 nm) following the method developed by Liz-Marzán's group,[16,17] as well as the subsequent upload and pH-controlled release of drugs for cancer therapy.[15] These different procedures can be combined in such a way

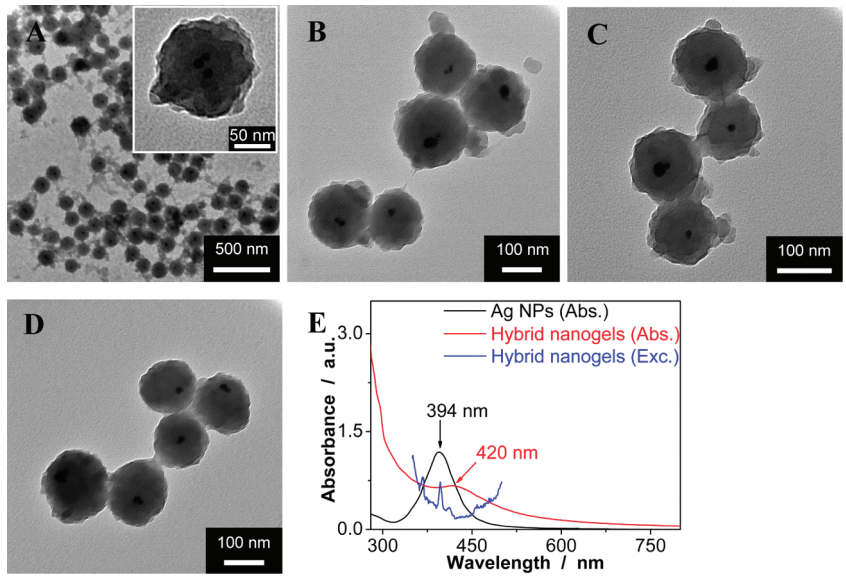

Figure 2. TEM images of the hybrid nanogels dried from the medium of pH = 7.4: (A) AVD-1, (B) AVD-2, (C) AVD-3, and (D) AVD-4. (E) Typical UV−vis absorption and excitation spectra of the hybrid nanogels. As a comparison, the absorption spectrum of the free Ag NPs is also presented.

that involves the first synthesis of SDS-capped Ag NPs (10 ± 3 nm), followed by the free-radical precipitation polymerization of the monomers to form a glucose responsive gel shell of a new copolymer p(VPBA−DMAEA) on the Ag NPs templates, so that the glucose-sensitive and fluorescent components can be integrated into a single nano-object. To avoid or minimize the formation of free nanogel spheres and to make sure that the Ag NP was encapsulated inside the hybrid nanogel, the concentrations of Ag NPs, SDS, and monomers were optimized for the one-step encapsulation of metal NPs within the p(VPBA−DMAEA) nanogel. With the similar Q values and the large difference in e values of VPBA ($Q = 0.38$, $e = -0.52$)[41] and DMAEA ($Q = 0.54$, $e = 0.61$)[42] monomers, the resulting p(VPBA−DMAEA) gel shell may possess alternating functional VPBA and DMAEA units through the network chains.

After the coating of the gel layer, the absorption peak of the Ag NPs red-shifted by ~26 nm (Figure 2E). This red-shift is related to a change in the local dielectric constant around the Ag NPs resulted from the coating of the p(VPBA−DMAEA) gel layer onto the Ag NPs.[17,43,44] As shown in Figure 2, the resultant core−shell particles have a spherical morphology with a very narrow size distribution (Supporting Information, Figure S1). The markedly high electron density of Ag enables direct visualization of the Ag NP core within the p(VPBA−DMAEA) nanogels. The hybrid nanogel synthesized with only VPBA but no DMAEA (as a control), coded as AVD-4, has the smallest size of only about 136 nm. After being copolymerized with DMAEA, the gel layer becomes thicker, and the thickness increases with the increase in DMAEA feeding. The hybrid nanogels AVD-3 (4.64 wt % DMAEA), AVD-2 (8.86 wt %) and AVD-1 (16.28 wt %) have an increased size of 139, 165, and 172 nm, respectively. The controllable size of the hybrid nanogels is very important to their fate in the bloodstream. Recognition by the reticuloendothelial system (RES) is known to be the principal reason for the removal of many colloidal drug carriers from the blood compartment.[45] The sub-200 nm size is desirable for colloidal particles to extend their blood circulation time.

The working pH is directed by the choice of functional groups in a glucose-sensing system, since the pK_a of the glucose receptor, here the phenylboronic acid (PBA) group, is an essential parameter for its selective binding and detection of glucose. Figure 3A shows the pH-induced volume phase transitions of the hybrid nanogels in terms of the change of hydrodynamic radius (R_h) measured at 37.2 °C. The pH-dependent phase behavior has been observed due to the presence of DMAEA (p$K_b \approx 7.5$) and VPBA (p$K_a \approx 8.9$) moieties. The amino groups in the pDMAEA segments were slightly ionized at the physiological pH and still not completely ionized at pH = 4.5. The swelling onset corresponding to the VPBA moiety in AVD-4 remained at about pH 8.8, whereas a decrease in the onset pH to about 7.8−8.0

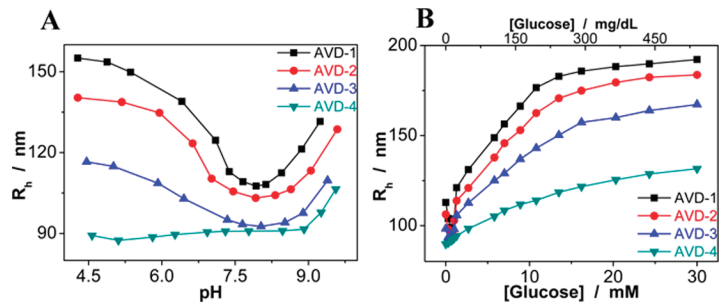

Figure 3. (A) pH-dependent average R_h values of the hybrid nanogels. (B) Glucose-dependent average R_h values, in PBS of pH = 7.38. All measurements were made at 37.2 °C and a scattering angle θ = 60°.

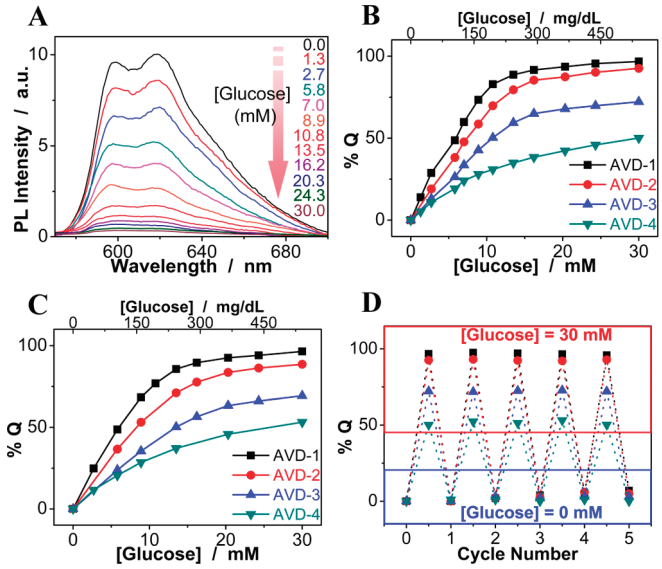

Figure 4. (A) Photoluminescence (PL) response of AVD-1 to glucose, showing typical evolution of the PL spectra. (B) Quenched PL at 618 nm as a function of the concentration of glucose. (C) Glucose response in the presence of 0.8 mM L-lactate. (D) PL quenching and recovery cycles upon the repeated addition (30.0 mM) and dialysis removal of glucose (0 mM) in the dispersion medium of the corresponding hybrid nanogels. All measurements were made in PBS of pH = 7.38 and 37 °C. Excitation wavelength = 492 nm.

was found in all other hybrid nanogels containing the DMAEA moiety. The PBA group is in equilibrium between the undissociated (trigonal, uncharged) and the dissociated (tetrahedral, charged) forms in aqueous solution.[20] Both forms react reversibly with 1,2-*cis*-diols such as glucose. The complexation of the uncharged form with glucose is unstable because it is highly susceptible to hydrolysis, but the binding of glucose induces the thermodynamically more favorable charged form. Two methods were previously proposed to enhance glucose recognition at physiological pH by either designing boronate analogues with lower pK_a values[21,22] or introducing intramolecular $B^{\delta-}\cdots X^{\delta+}$ bonds that confer a tetrahedral conformation at the boron center through the neighboring effect of an ortho group.[23,26,38] While sometimes the preparation protocols for the former are rigorous and time-consuming, the latter approach is more appealing. The presence of glucose can move the dissociation equilibrium of PBA to the right and further decrease its pK_a,[20] so if a strong intramolecular $B^{\delta-}\cdots X^{\delta+}$ bond can be generated, then such boronic acids would bind glucose at physiological pH. The effect of introducing a fixed positive charge in PBA hydrogel film was reported earlier by Horgan[25] and Lowe,[21] respectively, by using a quaternary amine of (3-acrylamidopropyl)trimethylammonium chloride (ATMA). In our design, a Lewis base DMAEA with small ionization, rather than a cation like ATMA, is demonstrated to be also useful to enhance the binding affinity of PBA to glucose at physiological pH range. The boronate ester in the hybrid nanogels is stabilized by electrostatic attraction ($B^-{-}N^+$) through the adjacent slightly protonated dimethyl amino groups, which should be stronger than the intramolecular interactions between boronate with neutral amide groups reported previously.[16,23,46,47]

Figure 3B shows that the swelling process of hybrid nanogels upon the addition of glucose can elegantly occur at pH = 7.4. The complexation of glucose with the hybrid nanogels increases the fraction of negatively charged boronates. At very low glucose concentrations (*e.g.*, < 0.75 mM), the complexation-induced negative charges on the boronates are electrostatically attracted to the slightly protonated DMAEA moieties in the hybrid nanogels, resulting in an initial decrease in R_h due to the charge neutrality (Supporting Information, Figure S2). On further increasing the glucose concentration, the overall charge of the hybrid nanogels changes from slightly positive to negative. The binding of glucose to the PBA increases the charge density on the gel and builds up a Donnan potential for the gel to swell steadily with an increase in glucose concentration. The swelling ratio, $R_{h,30\ mM}/R_{h,0\ mM}$, of AVD-1, AVD-2, and AVD-3 were found to be 1.71, 1.70, and 1.70, respectively, demonstrating the high sensitivity of these hybrid nanogels to glucose. In contrast, AVD-4 gave a much mild change in the overall response to glucose and a smaller $R_{h,30\ mM}/R_{h,0\ mM} = 1.46$, because the complexation of the uncharged PBA with glucose is unstable and it is highly susceptible to hydrolysis when the pH (= 7.4) is far below the pK_a (~8.9).

The glucose-responsive gel shell can modify the physicochemical environment of the Ag core NPs, converting biochemical signals into optical signals (Figure 4 and Supporting Information, Figure S3). As the size of Ag NPs is far smaller than the electron mean free path length (~50 nm),[46,47] robust photoluminescence (PL) can be detected from the hybrid nanogels dispersed in PBS at pH = 7.38. A slightly broadened absorption but a minimum of the excitation spectrum at the absorption peak of the hybrid nanogels (Figure 2E) can further confirm that plasmons do not make major contributions to the luminescence; rather, the luminescence likely arises from single-electron excitations between discrete energy states.[48,49] The PL of Ag core NPs is gradually quenched when the gel shell gradually swells up at the elevated glucose concentrations (Figure 4A,B). The comparison of Figure 4B with Figure 3B indicates that a conspicuous fluorescent response levels off at nearly the same glucose level where the gel network chains stretch to nearly a maximum. The linear plot (Supporting Information, Figure S4) gives the relationship in a more orthogonal fashion. The detection sensibility is estimated to be ±0.1 mM. The effect of the DMAEA moiety on the swelling ratio is also reflected in the fluorescent response, which shows that the incorporation of DMAEA has led to a much higher optical glucose sensitivity. It should be mentioned that glucose in the tested concentration range of 0−30 mM has

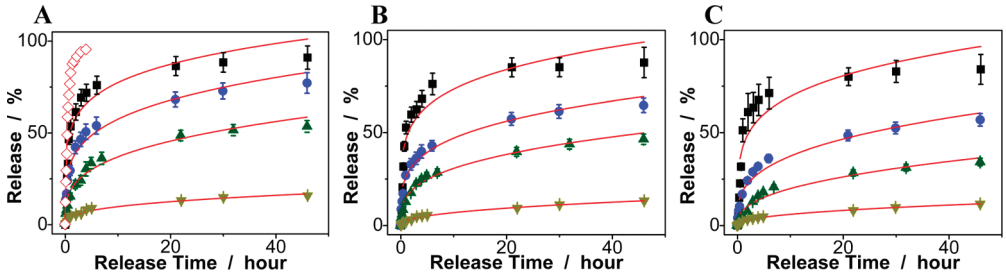

Figure 5. Releasing profiles of FITC-insulin from AVD-1 (A), AVD-2 (B), and AVD-3 (C), in the presence of 20 (■), 10 (●), 5 (▲), and 0 mM (▼) glucose in PBS of 7.38 at 37 °C. In the blank release (◇), the FITC-insulin solution was released to the PBS.

no effect on the fluorescence of free Ag NPs. One reason for this PL property change of Ag NP cores in the hybrid nanogels is associated with the variation of the Rayleigh scattering through the local refractive index change of the medium surrounding the Ag NPs, deriving from the volume phase transition of the gel shell.[17] The nonradiative energy loss paths, which are highly dependent on the nature of the environment around the metal particles,[50] possibly provide a second scenario for the fluorescence change. As the glucose concentration increases, the polymer chains tend to expand. However, the Ag core NPs offer the restoring force to hinder the network expansion, introducing an elastic tension in the bond at the polymer-Ag interface that would induce strain at the relaxed Ag NP surface,[51] creating interfacial states that quench the PL. The covalent bonds formed between the boronic acid and *cis*-diols are reversible.[20] As glucose is removed from the bathing medium by dialysis against very frequently changed water, the dissociation equilibrium shifts back from boronate ester to boronic acid, leading to a recovery of the fluorescence (93−96% and 99% of the original basal values for the hybrid nanogels containing and without DMAEA, respectively) upon the removal of glucose even after five cycles, thus providing a highly reproducible signal (Figure 4D), which is crucial for quantitative applications. This high reproducibility reflects the appropriate but not too great enhancement effect of DMAEA on the binding affinity of PBA to glucose. Since the changes in the optical properties of the Ag core NPs are caused by the glucose-induced volume phase transitions of the gel shell, the kinetics of the fluorescent response will depend on how quickly the nanogel shrinks or swells in response to a change in glucose concentration. It has been determined that the rate of the stimuli-induced volume phase transition of a hydrogel particle of 200−350 nm diameter is on the order of 100 ns.[52,53] We expect that the kinetics of the glucose-induced fluorescent response of our sub-200 nm hybrid nanogels should be on the hundreds nanosecond scale or even faster. One possible application of this optical feature is to noninvasively sense and image the glucose level within living systems.

Glucose sensors should be free from significant interferences from the nonglucose constituents of blood. The concentration of pyruvate, galactose, and fructose in blood is <0.1 mM,[54,55] thus it is unlikely that these compounds will interfere significantly with the glucose reading. However, the L-lactate concentration in a resting healthy adult is approximately 0.36−0.75 mM,[21,22,54,55] which could potentially be a significant interferent. In our design, the DMAEA group can stabilize the boronate anion which makes the attack of the boronic group by lactate unfavorable although the slightly positively charged DMAEA moiety will experience charge attraction on encountering lactate. As a result of the competitive effects on DMAEA, a decrease of 2−4% in glucose-induced PL quenching was observed in the presence of 0.8 mM L-lactate, corresponding to a 2−4% lower apparent concentration of glucose. On the contrary, the 0.8 mM lactate caused the non-DMAEA modified AVD-4 to indicate a ~7% higher apparent glucose concentration due to its competitive binding with the PBA. Clearly, the signaling ability of the DMAEA-containing hybrid nanogels provides excellent sensitivity and selectivity to glucose over lactate. The influence of metal ions on the glucose detection ability of the hybrid nanogels was also examined. The relative error of glucose concentration reading (0.4−20.0 mM) in the presence of 1.0 mM common metal ions found in biological systems, such as K^+ (−0.08%), Ca^{2+} (−0.23%), Na^+ (−0.05%), Mg^{2+} (−0.21%), Al^{3+} (−0.34%), Zn^{2+} (−0.23%), Fe^{3+} (−0.52%), and Cu^{2+} (−0.85%), is generally within the range of ±1% after taking account of the experimental errors. The slight interference from metal ions is possibly associated with the coordination between the metal ions and the boronic acid groups, or simply the enhancement of ionic strength. Both effects would weaken the Donnan potential.

Having demonstrated the signaling ability of the hybrid nanogels, we further applied them to the storage and delivery of insulin. The porous network structure of the gel shell is particularly well suited to trap insulin, resulting in a high drug loading capacity. The yields of FITC-insulin loaded into the hybrid nanogels were determined to be 38.3, 35.7, and 33.1 wt % (expressed as the mass of loaded drug per unit weight of dried hybrid nanogels) for AVD-1, AVD-2, and AVD-3, respectively. Considering the approximate concentrations of the

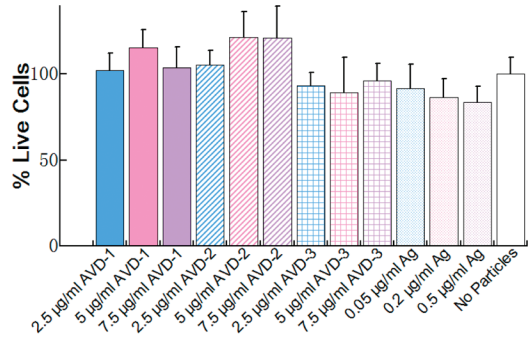

Figure 6. *In vitro* cytotoxicity of the hybrid nanogels and Ag NPs against Cos7 cells.

hybrid nanogel dispersions, these insulin loading capabilities are equivalent to 418.2, 404.3, and 428.4 IU/L, respectively. It should be noted that the hybrid nanogels can be concentrated and adjusted to an appropriate concentration to cover an even higher dose. Figure 5A−C shows the *in vitro* insulin releasing profiles from the hybrid nanogels measured by the dialysis method for 46 h in pH = 7.4 PBS at 37 °C. A blank release experiment of free FITC-insulin (~5800 Da) solution with an equivalent amount of drug to that trapped in AVD-1 was also performed, showing that the dialysis membrane (cutoff 12000−14000 Da) played a negligible role in the release kinetics. The much slower insulin release from the hybrid nanogels compared to the free drug solution indicates a sustained release process. The release can be further regulated by varying the glucose concentration in the releasing medium, demonstrating that the insulin could be released in a repeated on/off manner with fluctuating glucose level. At higher glucose levels (≥10 mM in diabetic patients), the DMAEA-containing hybrid nanogels can deliver a high amount of drug (56−91%, depending on the glucose concentrations and nanogel types), standing in vivid contrast with the low release efficiency of AVD-4 under the same conditions (Supporting Information, Figure S5). The time scales for insulin delivery are compatible with the patient's needs, since the DMAEA-containing hybrid nanogels could deliver insulin in less than 30 min, and the sustained release over 2 days may also meet the basal needs. Although the current results are obtained from *in vitro* studies, their characteristics for self-regulated insulin delivery could be extremely important in the treatment of diseases.

For future biological applications, the hybrid nanogels should be non- or low-cytotoxic. Assuming a required delivery of 1 mg/day (= 24 IU/day), the therapeutic amount of our hybrid nanogels need only be 1.5−4.0 mg after taking account of the release amount. A typical adult has a blood volume of between 4.7 and 5 L, with females generally having a smaller blood volume than males.[54,55] That is, the concentration of the hybrid nanogels could be less than 4 μg/mL used in the bloodstream. As shown in Figure 6, the hybrid nanogels were non- or low-cytotoxic to Cos7 cells after incubation for 24 h at concentrations of up to 7.5 μg/mL. Considering the possibility of degradation of the polymer gel during the long circulation, the potential cytotoxicity of free Ag NPs was also addressed. Once again, the free Ag NPs exhibit low cytotoxicity at all the studied concentrations.

CONCLUSIONS

We have designed an advanced glucose-sensitive platform with high sensitivity and selectivity at physiological pH and temperature on the basis of inorganic−organic core−shell structured hybrid nanogels. The beauty of this class of smart hybrid nanogels, which differentiates it from other examples of glucose sensors and nanoparticle-based insulin delivery systems, is the integration of glucose detection and self-regulated insulin delivery into a single nano-object. The chemical reagents and the developed hybrid nanogels are nontoxic to cells. The fluorescent functionality may allow noninvasive tracking of the distribution of the insulin carriers within the body. The multifunctional hybrid nanogels should promise a new efficient modality for single measurement of glucose concentrations, as well as for *in vivo* animal models and future clinical trials in diabetes management. We anticipate that the approach presented here may serve as a good starting point for the fabrication of multifunctional nanomaterials with a huge potential in biomedicine-related areas.

METHODS

Chemicals. All chemicals were purchased from Aldrich. 2-(Dimethylamino)ethyl acrylate (DMAEA) was purified with neutral Al_2O_3. The lyophilized fluorescein isothiocyanate-labeled insulin (FITC-insulin) from bovine pancreas (~5800 Da), sodium L-lactate, silver nitrate ($AgNO_3$), sodium citrate ($Na_3C_6H_5O_7 \cdot H_2O$), sodium borohydrate ($NaBH_4$), 4-vinylphenylboronic acid (VPBA), *N*,*N*′-methylenebisacrylamide (MBAAm), 2,2′-azobis(2-methylpropionamidine) dihydrochloride (AAPH), and sodium dodecyl sulfate (SDS) were used as received without further purification. The water used in all experiments was of Millipore Milli-Q grade.

Synthesis of Ag NPs. Citrate-stabilized Ag NPs were first prepared by dropwise addition of fresh $NaBH_4$ solution (10.6 mM, 2.5 mL) to an aqueous solution of $AgNO_3$ (0.1 mM, 200 mL) in the presence of sodium citrate (0.1 mM) under vigorous stirring. The resultant solution was stirred for 1 h and aged for 7 days at ambient conditions before use. The long aging time is necessary for completely degrading the reducing agent of $NaBH_4$. SDS-stabilized Ag NPs were obtained by adding 0.053 g SDS into 100 mL of aqueous solution of citrate-stabilized Ag NPs in a 250 mL round-bottom flask equipped with a stirrer, a N_2 gas inlet, and a condenser, and then aging the mixture for 10 h.

Synthesis of Ag@p(VPBA−DMAEA) Hybrid Nanogels. In a 250 mL round-bottom flask equipped with a stirrer, a N_2 gas inlet, and a condenser, 100 mL of as-prepared aqueous solution of SDS-stabilized Ag NPs was heated to 30 °C, followed by the addition of VPBA (0.970 g), DMAEA, and MBAAm (0.007 g) under stirring.

After 30 min, the temperature was raised to 70 °C and polymerization was initiated by adding 1 mL of 0.105 M AAPH. The polymerization reaction was allowed to proceed for 5 h. The solution was centrifuged twice at 6000 rpm (30 min, Thermo Electron Co. SORVALL RC-6 PLUS superspeed centrifuge) with the supernatant discarded and the precipitate redispersed in 200 mL deionized water. The resultant hybrid nanogels were further purified by 3 days of dialysis (Spectra/Por molecularporous membrane tubing, cutoff 12000−14000 Da MWCO, the same as below) against very frequently changed water at room temperature (~22 °C). The resultant hybrid nanogels made with the feeding of DMAEA = 0.20, 0.10, 0.05, and 0 mL are coded as AVD-1, AVD-2, AVD-3, and AVD-4, respectively.

Insulin Loading and Release. FITC-insulin was loaded to the hybrid nanogels by the complexation method. A stock solution of FITC-insulin (1 mg/mL) was prepared in 0.005 M phosphate buffer solution (PBS) of pH = 7.38, and stored in the refrigerator (4 °C). The pH value of the hybrid nanogel (5 mL) was adjusted to 9.0 by using dilute NaOH solution. This dispersion was stirred in an ice water bath for 30 min; 1 mL of FITC-insulin solution was then added dropwise to the vial. The immediate clouding revealed the hydrogen bonding complexation of the −OH groups in the insulin molecules with the boronic acid groups in the hybrid nanogels. After stirring overnight, the suspension was centrifuged at 6000 rpm for 30 min at 22 °C. To remove free drug, the precipitate was redispersed in 5 mL of PBS of pH = 7.38 and further purified by repeated centrifugation and washing. Finally, the precipitate was redispersed in 1 mL of PBS of pH = 7.38. All the upper clear solutions were collected, and the concentration of free drug was determined by fluorescence spectrometry at 518 nm upon excitation at 492 nm. The amount of loaded FITC-insulin in hybrid nanogels was calculated from the decrease in drug concentration. The loading content is expressed as the mass of loaded drug per unit weight of dried hybrid nanogels.

The *in vitro* release test of FITC-insulin from the hybrid nanogels was evaluated by the dialysis method. A dialysis bag filled with 1 mL of purified insulin-loaded hybrid nanogel dispersion was immersed in 50 mL of 0.005 M buffer solutions of pH = 7.38 at various glucose concentrations. The released FITC-insulin outside of the dialysis bag was sampled at defined time intervals and assayed by fluorescence spectrometry at 518 nm upon excitation at 492 nm. Cumulative release is expressed as the total percentage of drug released through the dialysis membrane over time. The release experiments were also performed to show the evolution of the release kinetics in response to glucose concentration changes.

***In Vitro* Cytotoxicity.** Cos 7 cells were plated in DMEM (Invitrogen, Carlsbad, CA) with 10% FCS at 10000 cells per well in two 96-well plates and allowed to grow overnight at 37 °C in 5% CO_2 incubator. The following day, the media were aspirated from the wells and the cells were treated with various concentrations of nanoparticles suspended in growing media, using three wells per concentration. The first plate was assayed 2 h after nanoparticle addition and the second one was assayed after 24 h. The percentage of DMEM and FCS was kept constant in each well. To estimate the amount of cell death, the wells were washed twice with phosphate-buffered saline, followed by the addition of 120 μL of 16.7% CellTiter 96 Aq_{ueous} One Solution (Promega, Madison, WI) in cell culture media in each well and further incubation at 37 °C in 5% CO_2. After 3.5 h, three portions of the solution obtained from each well were transferred to three respective wells of a 96-well plate. Absorbance was measured at 490 nm using a plate reader. Percentage of live cells was calculated relative to wells in same media conditions as the experimental wells but without any nanoparticles.

Characterization. The UV−vis absorption spectra were obtained on a Thermo Electron Co. Helios β UV−vis spectrometer. The PL spectra of the hybrid nanogel dispersions at various glucose concentrations were obtained on a JOBIN YVON Co. FluoroMax-3 spectrofluorometer equipped with a Hamamatsu R928P photomultiplier tube and a calibrated photodiode for excitation reference correction from 200 to 980 nm, with an integration time of 1 s. To confirm all emissions, the PL spectra were also recorded on a VARIAN CARY Eclipse fluorescence spectrophotometer equipped with R928 photomultiplier tubes and self-optimized light filters. The pH values were measured on a METTLER TOLEDO SevenEasy pH meter. The transmission electron microscopy (TEM) images were taken on a FEI TECNAI transmission electron microscope at an accelerating voltage of 120 kV. Approximately 10 μL of the diluted hybrid nanogel dispersion was air-dried on a carbon-coated copper grid for the TEM measurements. The hydrodynamic radius (R_h) was determined on a standard laser light scattering spectrometer (BI-200SM) equipped with a BI-9000 AT digital time correlator and a He−Ne laser (35 mW, 633 nm) as the light source. All hybrid nanogel dispersions were passed through Millipore Millex-HV filters with a pore size of 0.80 μm to remove dust before the DLS measurements.

Acknowledgment. This work is supported by the US Agency for International Development (PGA-P280422 for CUNY) and NSF CAREER award (MCB-0955407 for Yale). N. Mitra acknowledges the support from the Seessel Postdoctoral Fellowship.

Supporting Information Available: DLS size distributions, chemical structures, PL spectra, linear plot of quenched PL against glucose concentration, and release profiles of AVD-4. This material is available free of charge *via* the Internet at http://pubs.acs.org.

REFERENCES AND NOTES

1. Lim, S.I-Im.; Vaiana, C.; Zhang, Z.; Zhang, Y.; An, D. L.; Zhong, C. J. X-Shaped Rigid Arylethynes to Mediate the Assembly of Nanoparticles. *J. Am. Chem. Soc.* **2007**, *129*, 5368–5369.
2. Lim, S.I-Im.; Zhong, C. J. Molecularly-Mediated Processing and Assembly of Nanoparticles: Exploring the Interparticle Interactions and Structures. *Acc. Chem. Res.* **2009**, *42*, 798–808.
3. Qian, X.; Zhou, X.; Nie, S. M. Surface-Enhanced Raman Nanoparticle Beacons Based on Bioconjugated Gold Nanocrystals and Long Range Plasmonic Coupling. *J. Am. Chem. Soc.* **2008**, *130*, 14934–14935.
4. Qian, X.; Li, J.; Nie, S. M. Stimuli-Responsive SERS Nanoparticles: Conformational Control of Plasmonic Coupling and Surface Raman Enhancement. *J. Am. Chem. Soc.* **2009**, *131*, 7540–7541.
5. Nam, J.; Won, N.; Jin, H.; Chung, H.; Kim, S. pH-Induced Aggregation of Gold Nanoparticles for Photothermal Cancer Therapy. *J. Am. Chem. Soc.* **2009**, *131*, 13639–13645.
6. Jain, P. A.; Huang, X.; El-Sayed, I. H.; El-Sayed, M. A. Noble Metals on the Nanoscale: Optical and Photothermal Properties and Some Applications in Imaging, Sensing, Biology, and Medicine. *Acc. Chem. Res.* **2008**, *41*, 1578–1586.
7. Wiley, B.; Sun, Y.; Xia, Y. N. Synthesis of Silver Nanostructures with Controlled Shapes and Properties. *Acc. Chem. Res.* **2007**, *40*, 1067–1076.
8. Motornov, M.; Roiter, Y.; Tokarev, I.; Minko, S. Stimuli-Responsive Nanoparticles, Nanogels and Capsules for Integrated Multifunctional Intelligent Systems. *Prog. Polym. Sci.* **2010**, *35*, 174–211.
9. Zhang, Y.; Guan, Y.; Zhou, S. Q. Synthesis and Volume Phase Transitions of Glucose-Sensitive Microgels. *Biomacromolecules* **2006**, *7*, 3196–3201.
10. Hoare, T.; Pelton, R. Charge-Switching, Amphoteric Glucose-Responsive Microgels with Physiological Swelling Activity. *Biomacromolecules* **2008**, *9*, 733–740.
11. Lapeyre, V.; Ancla, C.; Catargi, B.; Ravaine, V. Glucose-Responsive Microgels with a Core−Shell Structure. *J. Colloid Interface Sci.* **2008**, *327*, 316–323.
12. Coakley, R. D.; Grubb, B. R.; Paradiso, A. M.; Gatzy, J. T.; Johnson, L. G.; Kreda, S. M.; O'Neal, W. K.; Boucher, R. C. Abnormal Surface Liquid pH Regulation by Cultured Cystic Fibrosis Bronchial Epithelium. *Proc. Natl. Acad. Sci. U.S.A.* **2003**, *100*, 16083–16088.
13. Helmlinger, G.; Yuan, F.; Dellian, M.; Jain, R. K. Interstitial pH and pO_2 Gradients in Solid Tumors *in Vivo*: High-

Resolution Measurements Reveal a Lack of Correlation. *Nat. Med.* **1997**, *3*, 177–182.
14. Zhu, M. Q.; Wang, L. Q.; Exarhos, G. J.; Li, A. D. Q. Thermosensitive Gold Nanoparticles. *J. Am. Chem. Soc.* **2004**, *126*, 2656–2657.
15. Wu, W.; Zhou, T.; Berliner, A.; Banerjee, P.; Zhou, S. Q. Smart Core−Shell Hybrid Nanogels with Ag Nanoparticle Core for Cancer Cell Imaging and Gel Shell for pH-Regulated Drug Delivery. *Chem. Mater.* **2010**, 1966–1976.
16. Contreras-Cáceres, R.; Sánchez-Iglesias, A.; Karg, M.; Pastoriza-Santos, I.; Pérez-Juste, J.; Pacifico, J.; Hellweg, T.; Fernández-Barbero, A.; Liz-Marzán, L. M. Encapsulation and Growth of Gold Nanoparticles in Thermoresponsive Microgels. *Adv. Mater.* **2008**, *20*, 1666–1670.
17. Álvarez-Puebla, R.; Contreras-Cáceres, R.; Pastoriza-Santos, I.; Pérez-Juste, J.; Liz-Marzán, L. M. Au@pNIPAM Colloids as Molecular Traps for Surface-Enhanced, Spectroscopic, Ultra-Sensitive Analysis. *Angew. Chem., Int. Ed.* **2009**, *8*, 138–143.
18. Yavuz, M. S.; Cheng, Y.; Chen, J.; Cobley, C. M.; Zhang, Q.; Rycenga, M.; Xie, J.; Kim, C.; Song, K. H.; Schwartz, A. G.; *et al.* Gold Nanocages Covered by Smart Polymers for Controlled Release with Near-Infrared Light. *Nat. Mater.* **2009**, *8*, 935–939.
19. Pickup, J. C.; Hussain, F.; Evans, N. D.; Rolinski, O. J.; Birch, D. J. S. Fluorescence-Based Glucose Sensors. *Biosens. Bioelectron.* **2005**, *20*, 2555–2565.
20. Davis, A. P.; Wareham, R. S. Carbohydrate Recognition through Noncovalent Interactions: A Challenge for Biomimetic and Supramolecular Chemistry. *Angew. Chem., Int. Ed.* **1999**, *38*, 2979–2996.
21. Yang, X.; Pan, X.; Blyth, J.; Lowe, C. R. Towards the Real-Time Monitoring of Glucose in Tear Fluid: Holographic Glucose Sensors with Reduced Interference from Lactate and pH. *Biosens. Bioelectron.* **2008**, *23*, 899–905.
22. Muscatello, M. M.; Stunja, L. E.; Asher, S. A. Polymerized Crystalline Colloidal Array Sensing of High Glucose Concentrations. *Anal. Chem.* **2009**, *81*, 4978–4986.
23. Ding, Z.; Guan, Y.; Zhang, Y.; Zhu, X. Layer-by-Layer Multilayer Films Linked with Reversible Boronate Ester Bonds with Glucose-Sensitive under Physiological Conditions. *Soft Mater* **2009**, *5*, 2302–2309.
24. Li, S.; Davis, E. N.; Anderson, J.; Lin, Q.; Wang, Q. Development of Boronic Acid Grafted Random Copolymer Sensing Fluid for Continuous Glucose Monitoring. *Biomacromolecules* **2009**, *10*, 113–118.
25. Horgan, A. M.; Marshall, A. J.; Kew, S. J.; Dean, K. E. S.; Creasey, C. D.; Kabilan, S. Crosslinking of Phenylboronic Acid Receptors as a Means of Glucose Selective Holographic Detection. *Biosens. Bioelectron.* **2006**, *21*, 1838–1845.
26. Hisamitsu, I.; Kataoka, K.; Okano, T.; Sakurai, Y. Glucose-Responsive Gel from Phenylborate Polymer and Poly(vinyl alcohol): Prompt Response at Physiological pH through the Interaction of Borate with Amino Group in the Gel. *Pharm. Res.* **1997**, *14*, 289–293.
27. Suri, J. T.; Cordes, D. B.; Cappuccio, F. E.; Wessling, R. A.; Singaram, B. Continuous Glucose Sensing with a Fluorescent Thin-Film Hydrogel. *Angew. Chem., Int. Ed.* **2003**, *42*, 5857–5859.
28. Peng, B.; Qin, Y. Lipophilic Polymer Membrane Optical Sensor with a Synthetic Receptor for Saccharide Detection. *Anal. Chem.* **2008**, *80*, 6137–6141.
29. Cordes, D. B.; Gamsey, S.; Singaram, B. Fluorescent Quantum Dots with Boronic Acid Substituted Viologens to Sense Glucose in Aqueous Solution. *Angew. Chem., Int. Ed.* **2006**, *45*, 3829–3832.
30. Tang, B.; Cao, L.; Xu, K.; Zhou, L.; Ge, J.; Yu, L. A New Nanobiosensor for Glucose with High Sensitivity and Selectivity in Serum Based on Fluorescence Resonance Energy Transfer (FRET) between CdTe Quantum Dots and Au Nanoparticles. *Chem.—Eur. J.* **2008**, *14*, 3637–3644.
31. Freeman, R.; Bahshi, L.; Finder, T.; Gill, R.; Willner, I. Competitive Analysis of Saccharides or Dopamine by Boronic Acid-Functionalized CdSe−ZnS Quantum Dots. *Chem. Commun.* **2009**, 764–766.
32. Gill, R.; Bahshi, L.; Freeman, R.; Willner, I. Optical Detection of Glucose and Acetylcholine Esterase Inhibitors by H_2O_2-Sensitive CdSe/ZnS Quantum Dots. *Angew. Chem., Int. Ed.* **2008**, *47*, 1676–1679.
33. Derfus, A. M.; Chan, W. C. W.; Bhatia, S. N. Probing the Cytotoxicity of Semiconductor Quantum Dots. *Nano Lett.* **2004**, *4*, 11–18.
34. Aslan, K.; Zhang, J.; Lakowicz, J. R.; Geddes, C. D. Saccharide Sensing using Gold and Silver Nanoparticles-A Review. *J. Fluoresc.* **2004**, *14*, 391–400.
35. Aslan, K.; Lakowicz, J. R.; Geddes, C. D. Nanogold Plasmon Resonance-based Glucose Sensing. 2. Wavelength-Ratiometric Resonance Light Scattering. *Anal. Chem.* **2005**, *77*, 2007–2014.
36. Lowman, A. M.; Morishita, M.; Kajita, M.; Nagai, T.; Peppas, N. A. Oral Delivery of Insulin Using pH-Responsive Complex-Ation Gels. *J. Pharm. Sci.* **1999**, *88*, 933–937.
37. Sajeesh, S.; Sharma, C. P. Cyclodextrin-Insulin Complex Encapsulated Polymethacrylic Acid Based Nanoparticles for Oral Insulin Delivery. *Int. J. Pharm.* **2006**, *325*, 147–154.
38. Lin, Y.; Mi, F.; Chen, C.; Chang, W.; Peng, S.; Liang, H.; Sung, H. Preparation and Characterization of Nanoparticles Shelled with Chitosan for Oral Insulin Delivery. *Biomacromolecules* **2007**, *8*, 146–152.
39. Shiino, D.; Murata, Y.; Kubo, A.; Kim, Y.; Kataoka, K.; Koyama, Y.; Kikuchi, A.; Yokoyama, M.; Sakurai, Y.; Okano, T. Amine Containing Phenylboronic Acid Gel for Glucose-Responsive Insulin Release under Physiological pH. *J. Controlled Release* **1995**, *37*, 269–276.
40. Zhao, Y.; Trewyn, B. G.; Slowing, I. I.; Lin, S. Y. Mesoporous Silica Nanoparticle-Based Double Drug Delivery Systems for Glucose-Responsive Controlled Release of Insulin and Cyclic AMP. *J. Am. Chem. Soc.* **2009**, *131*, 8398–8400.
41. Rzaev, Z. M. O.; Dinçer, S.; Pişkin, E. Functional Copolymer of *N*-Isopropylacrylamide for Bioengineering Applications. *Prog. Polym. Sci.* **2007**, *32*, 534–595.
42. Sideridou-Karayannidou, I.; Seretoudi, G. Synthesis and Characterization of Copolymers of *N*-Vinylcarbazole and *N*,*N*-Dimethylaminoethyl Acrylate. *Polymer* **1999**, *40*, 4915–4922.
43. Mulvaney, P. Surface Plasmon Spectroscopy of Nanosized Metal Particles. *Langmuir* **1996**, *12*, 788–800.
44. Schneider, G; Decher, G. From Functional Core/Shell Nanoparticles Prepared *via* Layer-by-Layer Deposition to Empty Nanospheres. *Nano Lett.* **2004**, *4*, 1833–1839.
45. Alexis, F.; Pridgen, E.; Molnar, L. K.; Farokhzad, O. C. Factors Affecting the Clearance and Biodistribution of Polymeric Nanoparticles. *Mol. Pharmaceutics.* **2008**, *5*, 505–515.
46. James, T. D.; Sandanayake, K. R. A. S.; Shinkai, S. Chiral Discrimination of Monosaccharides Using a Fluorescent Molecular Sensor. *Nature* **1995**, *374*, 345–347.
47. Zhu, L.; Shabbir, S. H.; Gray, M.; Lynch, V. M.; Sorey, S.; Anslyn, E. V. Astructural Investigation of the N−B Interaction in *o*-(*N*,*N*-Dialkylaminomethyl)arylboronate Systems. *J. Am. Chem. Soc.* **2006**, *128*, 1222–1232.
48. Kreibig, U.; Vollmer, M. In *Optical Properties of Metal Clusters*; Springer: Berlin, 1995; Vol. 25.
49. Zheng, J.; Ding, Y.; Tian, B.; Wang, Z. L.; Zhuang, X. W. Luminescent and Raman Active Silver Nanoparticles with Polycrystalline Structure. *J. Am. Chem. Soc.* **2008**, *130*, 10472–10473.
50. Wilcoxon, J. P.; Martin, J. E.; Parsapour, F.; Wiedenman, B.; Kelley, D. F. Photoluminescence from Nanosize Gold Clusters. *J. Chem. Phys.* **1998**, *108*, 9137–9143.
51. Wuister, S. R.; Doneg, C. M.; Meijerink, A. Luminescence Temperature Antiquenching of Water-Soluble CdTe Quantum Dots: Role of the Solvent. *J. Am. Chem. Soc.* **2004**, *126*, 10397–10402.
52. Wang, J.; Gan, D.; El-Sayed, M. A. Temperature-Jump Investigations of the Kinetics of Hydrogel Nanoparticle Volume Phase Transitions. *J. Am. Chem. Soc.* **2001**, *123*, 11284–11289.

53. Reese, C. E.; Mikhonin, A. V.; Kamenjicki, M.; Tikhonov, A.; Asher, S. A. Nanogel Nanosecond Photoic Crystal Optical Switching. *J. Am. Chem. Soc.* **2004**, *126*, 1493–1496.
54. Burtis, C. A.; Ashwood, E. R. *Tietz Textbook of Clinical Chemistry*, 3rd ed.; W.B. Saunders: Philadelphia, PA, 1999.
55. Cameron, J. R.; Skofronick, J. G.; Grant, R. M. *Physics of the Body*, 2nd ed.; Medical Physics Publishing: Madison, WI, 1999.